Physics in Medicine & Biology

IPEM Institute of Physics and Engineering in Medicine

Kill painting of hypoxic tumors with multiple ion beams

O Sokol[1], M Krämer[1], S Hild[2,3], M Durante[1,4] and E Scifoni[2]

[1] Biophysics Department, GSI Helmholtzzentrum für Schwerionenforschung GmbH, Planckstraße 1, D-64291 Darmstadt, Germany
[2] Trento Institute for Fundamental Physics and Applications (TIFPA-INFN), Via Sommarive 14, I-38123 Trento, Italy
[3] Department of Radiation Medicine and Applied Science, University of California San Diego, 9500 Gilman Drive, La Jolla, CA-92093, United States of America
[4] Technische Universität Darmstadt, Hochschulstraße 6, D-64289 Darmstadt, Germany

E-mail: m.kraemer@gsi.de

Abstract

We report on a novel method for simultaneous biological optimization of treatment plans for hypoxic tumors using multiple ion species. Our previously introduced kill painting approach, where the overall cell killing is optimized on biologically heterogeneous targets, was expanded with the capability of handling different ion beams simultaneously. The current version (MIBO) of the research treatment planning system TRiP98 has now been augmented to handle 3D (voxel-by-voxel) target oxygenation data. We present a case of idealized geometries where this method can identify optimal combinations leading to an improved peak-to-entrance effective dose ratio. This is achieved by the redistribution of particle fluences, when the heavier ions are preferentially forwarded to hypoxic target areas, while the lighter ions deliver the remaining dose to its normoxic regions. Finally, we present an *in silico* skull base chordoma patient case study with a combination of ^{4}He and ^{16}O beams, demonstrating specific indications for its potential clinical application. In this particular case, the mean dose, received by the brainstem, was reduced by 3%–5% and by 10%–12% as compared to the pure ^{4}He and ^{16}O plans, respectively. The new method allows a full biological optimization of different ion beams, exploiting the capabilities of actively scanned ion beams of modern particle therapy centers. The possible experimental verification of the present approach at ion beam facilities disposing of fast ion switch is presented and discussed.

1. Introduction

Radiotherapy with charged particles is one of the most rapidly growing branches of tumor treatment: in the last five years the number of patients, who received the corresponding treatment, had increased almost twice and now exceeds 150 000 (Jermann 2011, 2016, Durante *et al* 2017). Since the pioneering works at Berkeley in 1970s (Castro *et al* 1994, Castro 1995), the level of knowledge of physical and radiobiological properties of different ion beams has significantly improved. However, there is still a range of open challenges, aiming at its larger applicability and reducing cost-benefit ratio. Among them is the effective treatment of hypoxic tumors. Apart from the improvements in the computational and technical parts of the treatment planning and delivery, the efficiency and accuracy of the therapy can be improved for specific cases by introducing alternative ion modalities to the clinical practice. Nowadays, despite the fact that only two ion types (protons and carbon ^{12}C) are actually being used, there is a high interest towards implementing helium ^{4}He (Knäusl *et al* 2016, Krämer *et al* 2016, Tessonnier *et al* 2017) or oxygen ^{16}O (Kurz *et al* 2012, Dokic *et al* 2016, Sokol *et al* 2017) ions. Due to the decreased lateral scattering and still relatively low fragmentation tail behind the Bragg peak, ^{4}He beams are considered mainly as an alternative to protons, with promising indications especially for pediatric treatments (Knäusl *et al* 2016). At the same time, heavy ions, such as ^{16}O, having the increased linear energy transfer (LET) distribution over a broad range of a typical target (Tommasino *et al* 2016), can be beneficial for the treatment of hypoxic tumors. In the model study, published in our previous work Sokol *et al* (2017) we have shown that using ^{16}O for relatively low doses, prescribed to the tumors with the hypoxic areas of significant size, can lead to

improved sparing of the tissue in the beam entrance channel, compared to the lighter modalities, such as ^{4}He or ^{12}C, while for the normoxic targets the trend is opposite.

A further increase of the flexibility of ion beam treatment planning is expected to be achieved by simultaneously considering and optimally combining the physical and the radiobiological properties of several relevant ions simultaneously. The first clinical indication of the benefits of such a combined irradiation modality was the use of boost irradiations during the treatment of patients. In their study, Schulz-Ertner *et al* (2005) demonstrated almost a three-fold increase of the locoregional control after four years for patients with adenoid cystic carcinomas (ACC) treated between 1995 and 2003, who received a carbon boost in addition to the photon therapy, compared to those who received the photon treatment only. The explanation for this improvement was that for partially infiltrating tumors like ACC, carbon ions allow better coverage of the gross tumor volume, while photons irradiation in the boundary regions would have been safer.

The study of Böhlen *et al* (2013) proposed the idea of achieving a constant RBE inside the target by combining protons and carbon ions inside one treatment plan: the idea was to use the additional degree of freedom of the relative ratio of the different particles for imposing a minimum variation of the RBE, in the context of getting a more biologically robust plan. However, the price to pay was an increase of the cell killing in the beam entrance channel. Another idea, introduced in the same work, was the delivery of a heavy-ion boost to hypoxic regions of the target to achieve a constant biologically effective dose distribution. That idea arose from the previously published works on dose and LET painting methods, introducing the ideas of redistributing the particles LET during the treatment planning (Bassler *et al* 2010, Brahme 2011) (later followed by Bassler *et al* (2014), Malinen and Søvik (2015) and Unkelbach *et al* (2016)). In the meantime Krämer *et al* (2014) introduced for the first time the simultaneous optimization of different ion fields, and, for the hypoxia side, Scifoni *et al* (2013) and Tinganelli *et al* (2015) extended the LET painting approach with a full optimization driven process, based on the the local oxygenation, for a prescribed biological effect, e.g. survival level (kill painting).

The recent paper of Inaniwa *et al* (2017) demonstrated an alternative multiple ion strategy called intensity modulated composite particle therapy (IMPACT), which, using different particles simultaneously, enables the optimization of the dose and the LET distributions in a patient. However, no radiobiological models were included in the planning, and the optimization was carried out only for the absorbed dose. The patient study of Unkelbach *et al* (2018) revealed the benefit of a simultaneous use of several radiation modalities (protons and photons). However, the study was based on a heterogeneous fractionation schedule, and the explored degree of freedom was a different combination of single modality fractions. Moreover, no accounting for biological effects, including RBE, nor hypoxia was done in this case.

As of today, the only TPS capable of the simultaneous biological optimization of several different ion fields is TRiP98, the in-house TPS of GSI Heavy Ion Research Center. Krämer *et al* (2014) demonstrated a proof-of-concept example of such optimization with ^{12}C ions and protons for a C-shaped target representing the tumor wrapping an organ at risk (OAR). The system gave equal preference to both ions regarding the RBE-weighted dose for the large portion of the target. However, in the parts of the tumor in proximity to the OAR, the contribution of ^{12}C ion was more significant to achieve sharper dose fall-offs for better sparing of the OAR.

On the other hand, the version of TRiP98, presented by Scifoni *et al* (2013) and extended in Tinganelli *et al* (2015), using the above mentioned kill painting approach, can perform inverse planning aiming at the desired biological effect (or RBE-OER-weighted dose) in hypoxic tumors. However, this tool was not able to perform the optimization of several ion fields. Thus, the presented work was pursuing the goal of merging these two approaches realizing the first tool capable of the optimization with several primary ions accounting for tumor hypoxia.

In this paper, we report the results of the proof of concept study of multiple ion treatment planning for hypoxic tumors (or full multi-ion biological optimization, MIBO), as well as the following treatment planning study with a realistic patient geometry and artificially generated hypoxia map. The work is wrapped up with the discussion and conclusion sections which summarize the main results, explain the present limitations, and discuss necessary future steps.

2. Methods

The idea of the new treatment planning approach can be summarized as follows. The hypoxic parts of the tumor can be irradiated with heavier ions characterized by a higher LET as a function of depth: the high ionization density yields a lower oxygen enhancement effect and therefore an increased total biological effect compared to the lighter ion species. On the other hand, the remaining dose in the normoxic regions can be covered by the lighter ions, which results in less fragmentation and lower RBE values, thus allowing better sparing of the surrounding residual tissue and OARs.
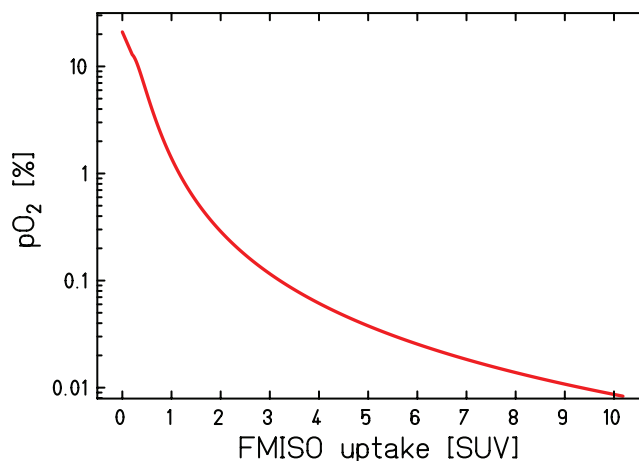
Figure 1. Visualization of the oxygenation lookup table generated according the model of Bowen *et al* (2011). The *x*-axis values correspond to the FMISO uptake signal in standardized uptake values (SUV) and the *y*-axis to the calculated pO_2 values.

2.1. TRiP98-MIBO

To enable a full biological optimization with multiple primary ion beams (MIBO), the calculation algorithms related to the OER interpolation and biological dose calculations, described by Scifoni *et al* (2013), were transferred to the current production version of TRiP98 (Krämer *et al* 2014) and partially improved. This implies changes in the calculation of the biological effect and improvement of the calculation of the dose gradients with respect to particle numbers, driving the optimization.

To enable handling of full 3D oxygenation maps (in the above mentioned previous studies we focused on monodimensionally varying oxygen profiles), the pO_2 data interpretation routine was updated. The new routine features the import of voxelized pO_2 datasets and an associated lookup table. The structure of the oxygenation map files and the procedure of its interpretation is similar to that for CT data and its Hounsfield units. This approach enables realistic *in silico* studies by allowing the user to load external clinical hypoxia map, originating, for example, from ^{18}F-FMISO scans, or to use the artificially generated pO_2 distribution cubes.

One of the commonly suggested approaches to obtain the oxygenation data is based on determining the uptake levels of the positron-emission tomography (PET) tracers (Horsman *et al* 2012), such as fluoromisoni-dazole (FMISO). For the studies, presented in this paper, the FMISO uptake-pO_2 lookup-tables were generated based on the model approach suggested by Bowen *et al* (2011). The corresponding uptake—pO_2 dependence is shown in figure 1.

2.2. Treatment planning studies

2.2.1. Simple geometry studies

For the proof-of-concept studies, the idealized geometry was chosen identical to the one used in Sokol *et al* (2017) for the comparative treatment planning study. A cubic water target volume of $40 \times 40 \times 60$ mm was placed at a center of a water cube of $200 \times 200 \times 160$ mm with isotropic 2 mm voxels. The LEM IV computed RBE tables for the CHO-K1 cell line, based on the linear-quadratic-linear model with x-ray response parameters $\alpha_X = 0.216$ Gy^{-1}, $\beta_X = 0.019$ Gy^{-2}, and transitional dose $D_T = 17$ Gy were chosen for the biological optimization. The choice of this cell line was determined by the fact, that this is the typical cell line used by our group for the previous *in vitro* plan verifications involving similar setups (Tinganelli *et al* 2015, Krämer *et al* 2016, Sokol *et al* 2017).

For the multiple-ion optimization studies, the size of the central hypoxic region of the target was set to 28 mm ($66 \leqslant z < 94$ mm) and had an oxygenation level of $pO_2 = 0.15\%$. The plan was optimized for two pairs of opposite fields of ^{4}He and ^{16}O for a uniform survival in the target of 10%, which corresponds to an isoeffective dose in hypoxia of $D_{isoh} = 6.5$ Gy(RBE, OER), where we define D_{isoh} as an RBE- an OER-weighted dose, voxel by voxel. The sketch of the geometry, the oxygenation distribution in the target, and the field directions are given in figure 2. The beam width (FWHM) was selected as 7 mm for ^{4}He beams and 5 mm for ^{16}O beams. For the combined plan, the scanner step sizes in *x*- and *y*-directions were set to 5 and 4 mm for ^{4}He and ^{16}O beams, respectively, while the distance between the subsequent peak positions was set as 3 mm for all fields. For the comparative single-ion plans with pure ^{4}He and ^{16}O, the scanner steps in *x*- and *y*-directions were set to 3 mm.

2.2.2. Patient plan study

For the study with a realistic patient geometry and more complex hypoxia distribution, the treatment plan data for a medium-sized skull base chordoma (planning target volume (PTV) of ≈ 133 cm^3) was chosen from
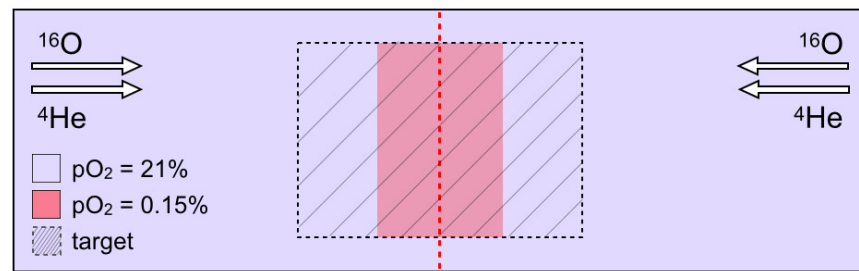
Figure 2. Schematic representation of geometry used for the simple geometry study. A rectangular target of $40 \times 40 \times 60$ mm (dashed area) was placed at a center of a water cube of $200 \times 200 \times 160$ mm. The oxygenation of the central region of 28 mm (red color) was assumed to be $pO_2 = 0.15\%$, and 21% for the rest of the volume (blue). Plan was optimized for two pairs of parallel-opposed fields of ^{4}He and ^{16}O.

the patient data archive of the GSI pilot project with ^{12}C ions (Schardt *et al* 2010). The field configuration was preserved from the original plan, and the couch angles were kept as 100 and -100 degrees, respectively.

This study also aimed at a comparison of a plan optimized for two pairs of ^{4}He and ^{16}O fields with the corresponding single-ion plans with double fields in the same geometry. The prescribed dose to the PTV was set to $D_{isoh} = 2$ Gy(RBE, OER). Similar to the original plan, the spinal cord was considered to be an organ at risk, with D_{max} per fraction $\leqslant 1.1$ Gy(RBE,OER) and a relative weight of 80% compared to target coverage. The LEM IV tables used for the planning were computed on the basis of the photon response curve for late toxicity in the central nervous system, with $\alpha/\beta = 2$ for both the tumor and residual tissue, similar as in Grün *et al* (2012) and Grün *et al* (2015). The pencil beam FWHM was selected as 5 mm for ^{16}O beams and 7 mm for ^{4}He beams. The scanner steps in x- and y-directions were set to 2 and 3 mm for the single-ion ^{16}O and ^{4}He plans, respectively, and 4 mm for each field in the combined plans.

The artificially modeled pO_2 map represents a series of differently oxygenated isocentric regions, where each of the contours is a shrunk contour of the original tumor (GTV). The shrinkage was done using the 3D Slicer software (Kikinis *et al* 2014). The emulated oxygenation is decreasing from 21% to 0% from the edges of the PTV towards its center. Such a distribution, even if arbitrary and exemplary, is consistent with many reported profiles in functional PET measurements (Thorwarth *et al* 2007, Horsman *et al* 2012). Figure 3 illustrates the patient geometry, emulated hypoxia distribution, and field configuration in proximal, coronal, and sagittal views.

3. Results

3.1. Proof of concept of 3D kill painting

Prior to the multi-ion optimization studies, a short study using the artificially generated pO_2 map was done for the cubic geometry described above to test if the system is able to handle the 3D oxygenation data properly. The emulated ellipsoid pO_2 distribution is presented in figure 4(a). The oxygenation is gradually decreasing from 21% until 0% towards the target center.

Figures 4(b)–(e) show the results of the optimization of two parallel-opposed fields of ^{16}O beams using kill painting approach for a uniform survival of 10% in the target region. The resulting uniform biological (RBE- and OER-weighted) dose and the cell survival (figures 4(b) and (e), respectively) are achieved by delivering the physical dose boost to the central target part (figure 4(c)). The 1D cuts along the line running through the center of CT for the resulting optimized dose and dose-averaged LET cubes are presented in figures 5(a) and (b), respectively.

Most importantly, we notice that the dose-averaged LET distribution ($\overline{LET}$, defined as in Tinganelli *et al* (2015) as the sum of the LET of all the individual particles composing the beam weighted for their relative doses) is automatically adjusted in 3D to the oxygenation, achieving its maximum in the most hypoxic target part, as illustrated in figure 4(d). One may notice that the area of the relatively high values of $\overline{LET}$ extends beyond the target borders in lateral directions. The explanation of this effect can be the presence of the few high-LET particles delivering a very low total dose in this region; a similar effect can be observed in the studies of Bassler *et al* (2014).

Thus, we demonstrate that the kill painting efficiency in LET redistribution, already demonstrated in 1D in Krämer *et al* (2014) is also working in 3D. It is important to recall that $\overline{LET}$, being a dose averaged distribution cannot be scaled arbitrarily as the dose, rather it can be re-distributed across a target. Thus, we achieve an effect similar to LET painting, but without imposing any dose ramp by construction.

3.2. Model volume study

The 1D cuts along the line running through the CT center for the resulting optimized RBE-OER-weighted dose and dose-averaged LET cubes are presented in figures 6(a) and (b), respectively. For this study, the oxygenation
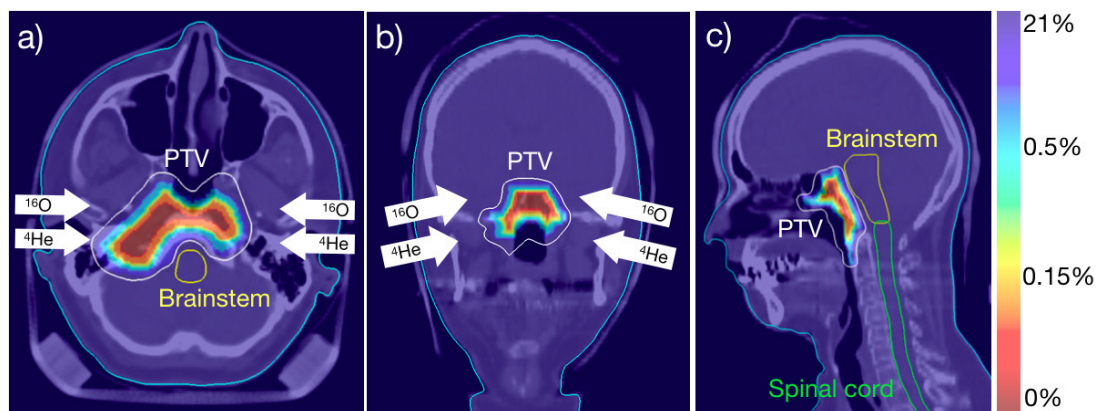
Figure 3. Artificially generated hypoxia map for the studied case of skull base chordoma in (a) proximal, (b) coronal, and (c) sagittal views. The couch angles were set to 100 and −100 degrees. The contours of the planned tumor volume, the brainstem and the spinal cord are outlined with white, yellow and green lines, respectively. The color scale represents the oxygenation gradient decreasing from $pO_2 = 21\%$ to $pO_2 = 0\%$.
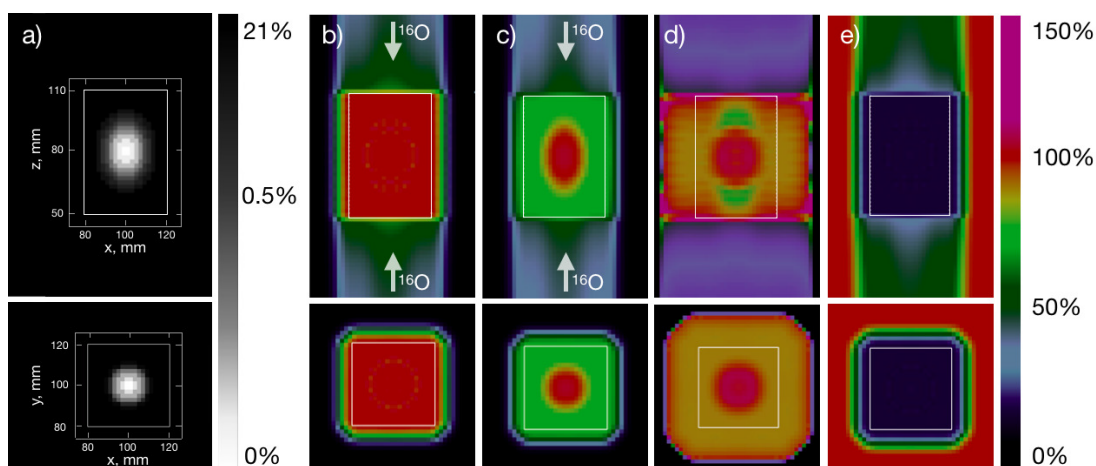

Figure 4. (a) Emulated hypoxia map, pO_2 is decreasing towards the target center. (b)–(e) Plan optimized for a uniform survival of 10% in a target, irradiated with two parallel-opposed fields of ^{16}O ions. (b) RBE-OER-weighted dose, (c) absorbed dose, (d) dose-averaged LET, and (e) survival distributions. In (b) and (c) 100% of the scale stands for the dose of 6.5 Gy, in (d) for the LET of 100 keV μm^{-1}, in (e) for the 10% survival. Top and bottom rows correspond to the coronal and axial panes, with target area marked with white lines.
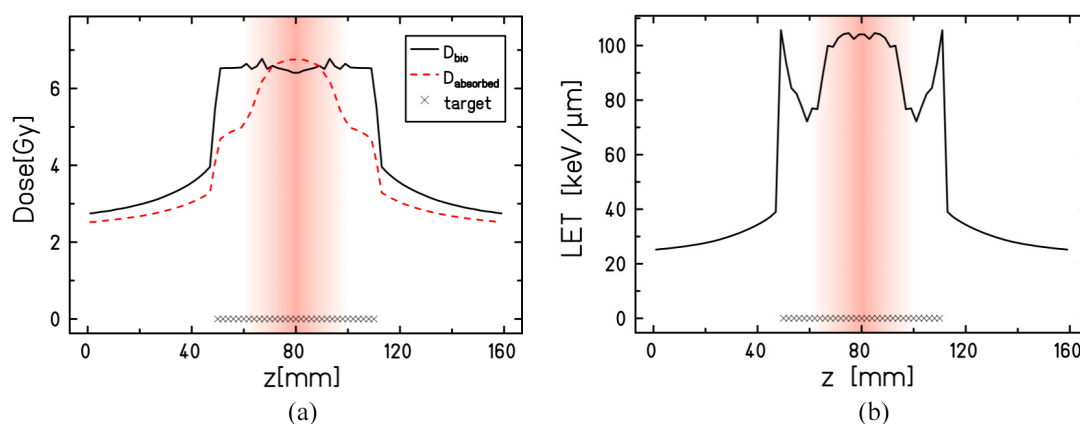
Figure 5. Results of the plan optimization for two parallel-opposed fields of ^{16}O ions for a uniform target survival of 10%. The 1D cuts along the central line of the geometry are shown. The hypoxic region with oxygenation decreasing from 21% to 0% is shown with a color gradient (white color corresponds to $pO_2 = 21\%$ and red colour—to $pO_2 = 0\%$). The target region is marked with crosses. (a) RBE- and OER- weighted dose (D_{bio}) and absorbed dose distributions. (b) Dose-averaged LET profile.
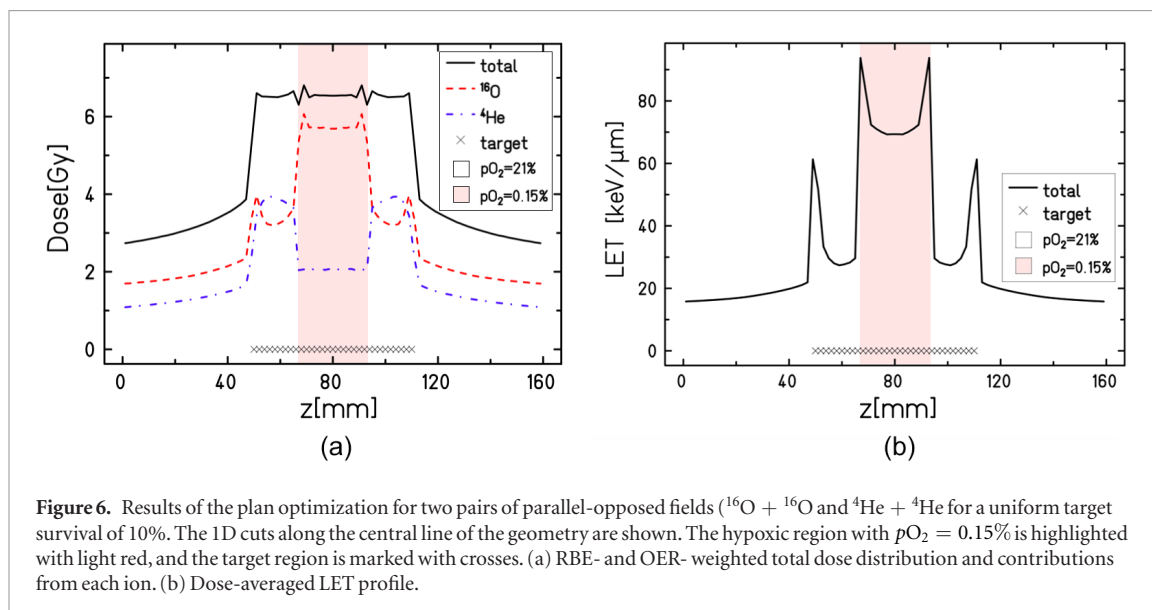
Figure 6. Results of the plan optimization for two pairs of parallel-opposed fields (^{16}O + ^{16}O and ^{4}He + ^{4}He for a uniform target survival of 10%. The 1D cuts along the central line of the geometry are shown. The hypoxic region with $pO_2 = 0.15\%$ is highlighted with light red, and the target region is marked with crosses. (a) RBE- and OER- weighted total dose distribution and contributions from each ion. (b) Dose-averaged LET profile.
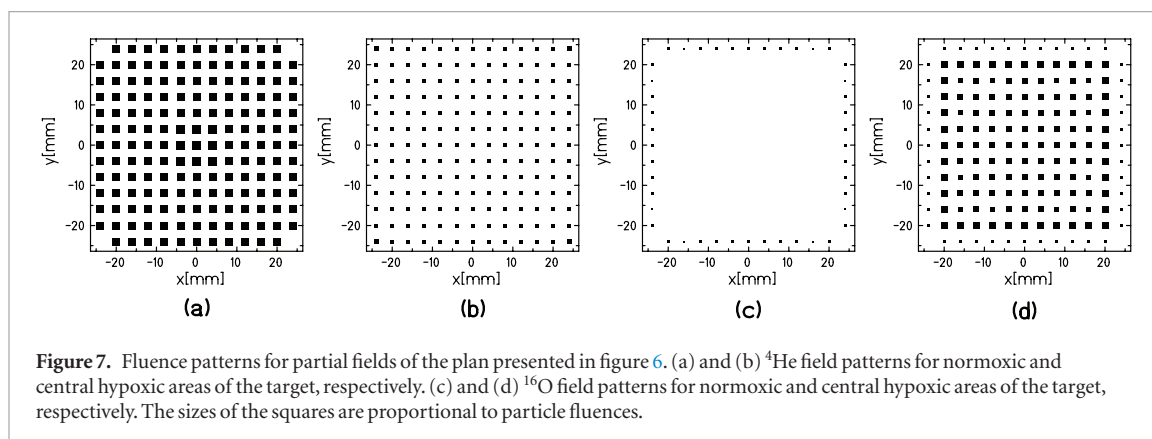

Figure 7. Fluence patterns for partial fields of the plan presented in figure 6. (a) and (b) ^{4}He field patterns for normoxic and central hypoxic areas of the target, respectively. (c) and (d) ^{16}O field patterns for normoxic and central hypoxic areas of the target, respectively. The sizes of the squares are proportional to particle fluences.

levels in the target were set to 0.15% in the central area ($66 \leqslant z < 94$ mm), and 21% in the remaining parts. As one can see from the RBE-OER-weighted dose profiles (figure 6(a)), to achieve the uniform survival, ^{16}O generates a high-dose and thus also high LET 'boost' in the hypoxic region, while in the remaining normoxic areas its contribution is almost equal to the one of ^{4}He, with a slight overweight of the contribution of the latter ion. The resulting increased $\overline{\text{LET}}$ distribution reaches its maximum of 95 keV μm^{-1} at the borders of the hypoxic region, being always over 70 keV μm^{-1} in the rest of the target, as shown in figure 6(b). According to the model of Scifoni *et al* (2013), this should lead to a reduction of OER from ≈ 2 down to ≈ 1.5. The 'spikes' in the $\overline{\text{LET}}$ distribution on the target borders are caused by stopping particles, and inside the target they appear due to the drastic changes of oxygenation.

For providing a more detailed insight into the fields redistribution, the fluence patterns for the single-field contributions of each ion are given in figure 7. The first two figures correspond to the fluence patterns of ^{4}He beams with initial energies of 121.68 (a) and 109.97 MeV u^{-1} (b), stopping in normoxic and hypoxic regions of the tumor, respectively. Figures 7(c) and (d) describe the patterns for ^{16}O beams with energies 271.59 and 244.15 MeV u^{-1}, respectively. The sizes of the squares are proportional to the particle numbers per spot. Thus, the fluence of ^{4}He decreases more than twice, from 3.6–3.7 $\times$ 10^6 per spot in the normoxic areas to $\approx$1.8 $\times$ 10^6 per spot in the hypoxic center. In contrast, ^{16}O is almost avoided in the normoxic region, contributing to the dose only at the edges of the target, and is mainly concentrated in the hypoxic part (6–7 $\times$ 10^5 particles per spot).

The resulting ion contributions can be further adjusted by introducing an additional constraint on the beam energies, selected during the optimization, in order to explore a 'limit' situation. This way, one can further decrease the presence of stopping ^{16}O beams in normoxic areas, and ^{4}He in hypoxic. For example, for a given treatment plan the ^{16}O energies can be selected in the range of 221.53–254.99 MeV u^{-1}, ensuring the beam ranges are $\approx$ 74–95 mm, and 115.93–124.78 MeV u^{-1} for ^{4}He, corresponding to the ranges of 97–112 mm. The resulting cell survival, calculated for the plan, adjusted accordingly, is shown in figure 8. From the comparison with the single-ion double-field ^{4}He and ^{16}O plans it can be concluded, that the combined strategy can reduce the damage to the residual tissue in the beam path. Additionally, in figure 8 the numerical values of the respective
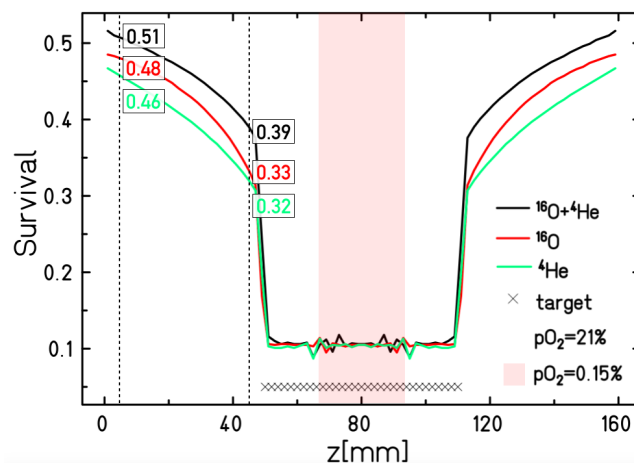
Figure 8. One-dimensional survival distributions for the combined four-field $^{16}O + {}^4He$ plan, and two-field single-ion ^{16}O and ^4He plans in opposed field directions (see figure 2). The hypoxic region with $pO_2 = 0.15\%$ is highlighted with light red, and the total target region is marked with crosses.
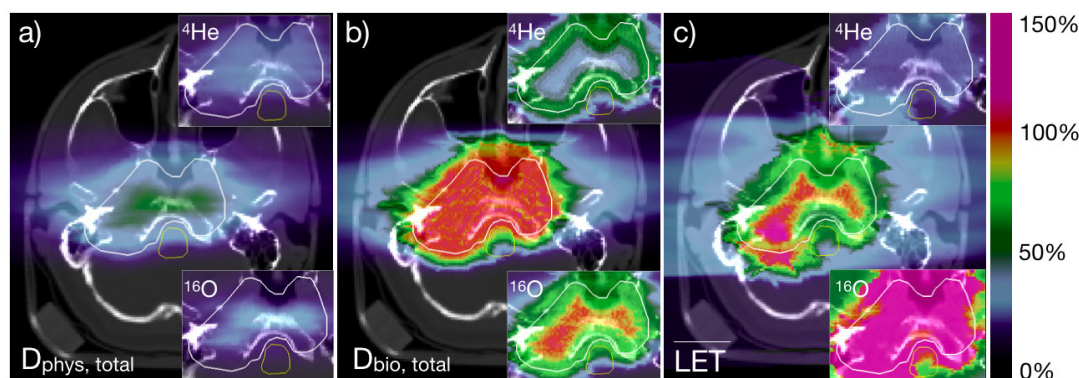
Figure 9. Biologically optimized four-field $^{16}O + {}^4He$ plan for a partially hypoxic skull base chordoma (see figure 3 for detailed oxygenation profile and morphological description). (a) Total physical dose, insets correspond to the partial contributions from ^{16}O and ^4He fields. (b) Total biological (RBE-OER-weighted) dose, insets correspond to the partial contributions from ^{16}O and ^4He fields. (c) Dose-averaged LET distribution, insets correspond to the partial contributions from ^{16}O and ^4He fields. For (a) and (b) the color scale represents the relative dose compared to the dose of 2 Gy, for (c) the relative LET compared to the LET of 60 keV μm^{-1}.

survival rates for the residual tissue at depths of 5 mm (beam entrance channel) and 45 mm (the proximity of a target) are provided. Thus, for this particular geometry and oxygenation the improvement in the cell survival in the entrance channel, compared to the single-ion ^4He and ^{16}O plans, is 11% and 6% at a depth of 5 mm, and 22% and 18% at 45 mm, respectively.

3.3. Patient plan study

The resulting absorbed dose, RBE-OER-weighted dose and dose-averaged LET distributions on a central axial slice for a combined plan are given in figures 9(a)–(c), respectively. Additionally, the contributions from each ion are added to the first two figures. Similar to the plans in the previous section, most of the dose to the hypoxic areas is delivered by ^{16}O ions, while the contribution from ^4He plays a role only in normoxic parts. The dose-averaged LET values are increasing from the edges towards the anoxic center of the PTV, reaching the maximum of ≈ 73 keV μm^{-1}, thus reducing the OER in the target from ≈ 2.7 down to ≈ 2.1. Since, according to our model (Scifoni *et al* 2013), OER starts to decrease at the LET values of 50–60 keV μm^{-1}, we chose the value of 60 keV μm^{-1} as 100% for the colour scale of figure 9(c).

As follows from the spatial location of the spinal cord and brainstem, relative to the target, the dose they receive is mainly caused by either beam fragmentation in case of pure ^{16}O plan, or by lateral scattering in case of a pure ^4He plan. Thus, the field redistribution in case of a combined plan can potentially lead to the reduction of fragmentation and scattering in the proximity of the target.

The quality of the analyzed single-ion and combined treatment plans was assessed using the dose-volume histograms (DVH) for the RBE-OER-weighted doses. The resulting DVHs for the target, the spinal cord, and the
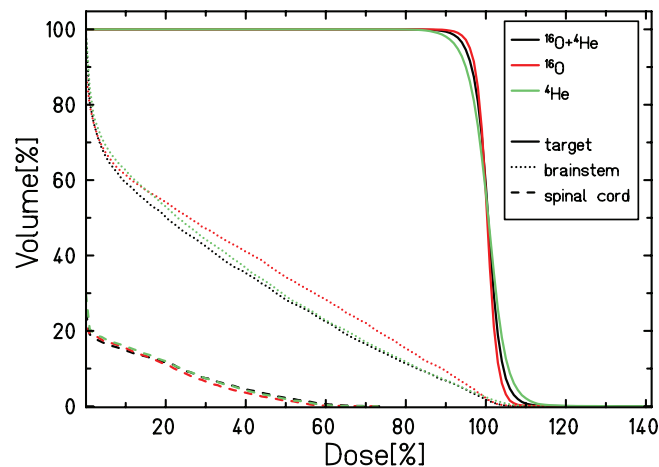
Figure 10. Dose-volume histograms for the target (solid lines), brainstem (dotted lines) and spinal cord (dashed lines) for the plans, optimized for a uniform RBE-OER-weighted dose of 2 Gy in the target. Black lines: combined four-field ^{16}O and ^{4}He plan; red: two-field ^{16}O plan; green: two-field ^{4}He plan.

brainstem for all simulated plans are shown in figure 10. Although the brainstem was not set as an OAR in the original plan, it receives a significant dose; thus the effect of the combined plan on it has been assessed as well.

The deviations in the mean dose received by the PTV do not exceed 4.5% from the prescribed value of 2 Gy for any of the analyzed plans. The fluctuations in the target dose are mainly observed at the borders of differently oxygenated regions and are caused by the changes of pO_2 from voxel to voxel; in realistic cases, the pO_2 is expected to vary in a smoother fashion, thus leveling these discontinuities. As can be seen from the DVH, the dose to the brainstem for the combined plan is slightly reduced compared to the single-ion plans. The respective mean dose (0.62 Gy) is lower by 10%–12% as compared to the pure ^{16}O plan (0.71 Gy) and 6%, compared to the ^{4}He plan (0.66 Gy). The mean dose to the spinal cord remains intermediate as compared to the single-ion plans and does not exceed the value of 0.1 Gy for all of them. The dose received by residual tissue is not illustrated by the respective DVH. Only a very small volume of residual tissue, compared to the total, has received any dose, and for all the plans the respective mean dose is ≈ 0.028 Gy. It is important to mention here, that no constraints on the energy selection during optimization were applied, thus the optimal arrangement of particles and overall LET distribution is automatically realized by the TPS.

4. Discussion

The modifications to the TRiP98 planning system introduced here make it the only research TPS able to calculate the biological effect of several ion beams simultaneously in one treatment plan, by optimizing their contributions accounting for the target oxygenation. It is important to note, that in contrast to a pure LET painting approach, as in Bassler *et al* (2014) and Inaniwa *et al* (2017), where the high-LET particles (and/or the high-LET components of a beam) are by construction imposed in the particular regions of a target, in the kill painting and explicitly in this present implementation, the particle type and the particle fluences are optimally chosen automatically by the TPS based on the 3D hypoxic imaging input.

The multiple-ion strategy has to be chosen wisely, since, apart from the generally longer optimization time and slightly increased irradiation times, it might worsen the treatment outcome, compared to the corresponding single-ion plans. Our previous study (Sokol *et al* 2017) has demonstrated that lighter ions deliver the lower doses in the entrance channel in case of normoxic tumors, while the benefit of heavier ions is elevated by larger hypoxic regions and/or general decrease of oxygenation. Thus, one should not expect to further reduce damage in the entrance channel by adding heavy ions to a light-ion plan in case of almost normoxic tumors. On the other hand, the inclusion of the light ions to plans with ^{12}C or ^{16}O beams may counteract the quality of the plan for very hypoxic tumors. In the simple geometry study, demonstrated in section 3.2, an intermediate size of a hypoxic area was modeled, when, according to our previous analysis, the outcome of the ^{16}O plan is expected to perform only slightly better, than for ^{4}He plan. The manual energy selection approach, used to tune the outcome of the respective multiple-ion plan, is not applicable for treatment planning with irregular and asymmetric patient geometries. However, it can be interpreted as an 'asymptotic' case and can serve as a guide for the further improvement of the optimization mechanisms.

The experimental biological verification of the multiple-ion treatment planning is essential and is one of the main directions of the further work. Apart from the general estimation of the planning reliability, it is necessary to make sure the slightly increased time of the irradiation session and dose fractionation do not affect the bio-

logical effects (e.g. repair processes). The precision of the particle range determination is another issue of high importance for the combined planning. Since the redistribution of the fields is expected to occur in the different regions of the tumor, the positioning of the patient and the calculations of the ranges of all the primaries have to be done with a high degree of accuracy. Thus, robustness assessment of these plans will be certainly the subject of future studies.

The treatment plans, presented here, were analyzed for the case of parallel-opposed fields (model studies) or fields coming at very small angles (patient plan study), while in some clinical cases this field configuration may be contraindicated. While using the parallel-opposed field configuration one can take the most out of the LET effect, other field configurations together with multi-ion approach still might be beneficial depending on the specific spatial location of tumor and organs at risk. Investigation of such cases is another subject left for the future studies.

In general, a clinical application of the multi-ion approach, despite being very challenging, appears to be realistic. For example, at the Heidelberg ion beam therapy center the switching from one ion type to another one coming from the same source (from ^{16}O to ^{12}C, or vice versa) already takes not more than 10 min. Moreover, since the approach implies the usage of different ion combinations, e.g. $^{16}O + {}^4He$, the switching time is expected to be decreased further since there are different sources for these ions running continuously. Recently, in his talk Furukawa (2017) reported that Toshiba managed to achieve a switching time between two ions within one source to be less than a minute, and they are going to implement this in the Japanese facilities; moreover, they are aiming at reducing this to 5 s, i.e. on a pulse-by-pulse level. Since the dose is split between several fields, the irradiation with each of them will be shorter. This way, the total irradiation time is expected to exceed the one in case of standard single-ion treatment mainly by the time required to rotate the patient. For the studies presented here, only four-fields multi-ion plans were investigated, however, in other cases, a reduced number of multiple-ion fields might be more beneficial.

The difficulty to obtain a proper and sufficiently resolved oxygenation map of a tumor tissue, also accounting for its rapid temporal variation in the course of a treatment, considering the limitation of the present techniques (functional PET and MRI), has to be mentioned as one of the main limitations of any dose, LET or kill painting methods. Robust accounting for a rapidly varying oxygen distribution is thus, of course, another subject of further investigation. Nevertheless, what we provide is a tool which is able to account for this oxygenation induced heterogeneity, and, once this is available, to adapt the plan accordingly.

5. Conclusions

The multiple-ion full biological optimization (MIBO) approach, introduced in this work, aims at improving the treatment planning of tumors with heterogeneous oxygen status by using multiple ion beams with different capabilities to kill hypoxic cells. This includes the decreased fragmentation of the light ions or the higher RBE and LET values of the heavier ions. As both the simple geometry and patient studies have shown, the uniform biological effect is achieved by forwarding the heavier ion modalities to hypoxic regions of the target while covering the normoxic areas preferably with lighter ions. This allows one to increase the dose-averaged LET distribution in hypoxic parts to reduce the OER while avoiding the high $\overline{LET}$ where it is not necessary.

In this contribution, we studied combined $^{16}O + {}^4He$ plans, since both these ions are mostly discussed nowadays as the alternatives to the well-established ^{12}C and ^1H, respectively. Performing the further multiple-ion tests involving other ions apart from ^{16}O and ^4He is one of the further directions of this work. Since ^{12}C currently is more widely used than ^{16}O, further studies on the combination of $^{12}C + {}^1H$ should follow.

In the example with the skull-base chordoma, it was shown that applying a four-field combined plan allows reducing the mean dose to the brainstem by 3%–5% compared to the pure ^4He plan and by 10%–12% compared to the pure ^{16}O plan. At the same time, this plan is beneficial regarding the maximal dose to the OAR, since it always remains as low as possible, meaning it being similar as for the ^4He plan in normoxia and as for ^{16}O plan in hypoxia. This study was carried out with an artificially generated hypoxia map. More realistic studies should involve real PET hypoxia maps obtained from clinical cases.

Acknowledgments

ORCID iDs

M Durante ⬤ https://orcid.org/0000-0002-4615-553X

References

Bassler N, Jäkel O, Søndergaard C S and Petersen J B 2010 Dose- and LET-painting with particle therapy *Acta Oncol.* **49** 1170–6

Bassler N, Toftegaard J, Lühr A, Sørensen B S, Scifoni E, Krämer M, Jäkel O, Mortensen L S, Overgaard J and Petersen J B 2014 LET-painting increases tumour control probability in hypoxic tumours *Acta Oncol.* **53** 25–32

Böhlen T T, Bauer J, Dosanjh M, Ferrari A, Haberer T, Parodi K, Patera V and Mairani A 2013 A Monte Carlo-based treatment-planning tool for ion beam therapy *J. Radiat. Res.* **54** i77–81

Bowen S R, van der Kogel A J, Nordsmark M, Bentzen S M and Jeraj R 2011 Characterization of positron emission tomography hypoxia tracer uptake and tissue oxygenation via electrochemical modeling *Nucl. Med. Biol.* **38** 771–80

Brahme A 2011 Accurate description of the cell survival and biological effect at low and high doses and LET's *J. Radiat. Res.* **407** 389–407

Castro J R 1995 Results of heavy ion radiotherapy *Radiat. Environ. Biophys.* **34** 45–8

Castro J R, Linstadt D E, Bahary J P, Petti P L, Daftari I, Collier J, Gutin P H, Gauger G and Phillips T L 1994 Experience in charged particle irradiation of tumors of the skull base: 1977–1992 *Int. J. Radiat. Oncol. Biol. Phys.* **29** 647–55

Dokic I, Mairani A, Niklas M, Zimmermann F, Jäkel O, Debus J, Haberer T and Abdollahi A 2016 Next generation multi-scale biophysical characterization of high precision cancer particle radiotherapy using clinical proton, helium-, carbon- and oxygen ion beams *Oncotarget* **7** 56676–89

Durante M, Orecchia R and Loeffler J S 2017 Charged-particle therapy in cancer: clinical uses and future perspectives *Nat. Rev. Clin. Oncol.* **14** 483

Furukawa T 2017 Technological advancements translated to clinical advantages *Talk Presented at Int. Symp. on Ion Therapy (Dallas, 2 November 2017)*

Grün R, Friedrich T, Elsässer T, Krämer M, Zink K, Karger C P P, Durante M, Engenhart-Cabillic R and Scholz M 2012 Impact of enhancements in the local effect model (LEM) on the predicted RBE-weighted target dose distribution in carbon ion therapy *Phys. Med. Biol.* **57** 7261–74

Grün R, Friedrich T, Krämer M, Zink K, Durante M, Engenhart-Cabillic R and Scholz M 2015 Assessment of potential advantages of relevant ions for particle therapy: a model based study *Med. Phys.* **42** 1037–47

Horsman M R, Mortensen L S, Petersen J B, Busk M and Overgaard J 2012 Imaging hypoxia to improve radiotherapy outcome *Nat. Rev. Clin. Oncol.* **9** 674–87

Inaniwa T, Kanematsu N, Noda K and Kamada T 2017 Treatment planning of intensity modulated composite particle therapy with dose and linear energy transfer optimization *Phys. Med. Biol.* **62** 5180–97

Jermann M 2011 Hadron therapy patient statistics (data recieved per May 2011; PTCOG50) www.ptcog.ch/archive/patient_statistics/Patientstatistics-updateMay2011.pdf

Jermann M 2016 Particle therapy patient statistics (per end of 2015) www.ptcog.ch/archive/patient_statistics/Patientstatistics-updateDec2015.pdf

Kikinis R, Pieper S D and Vosburgh K G 2014 3D slicer: a platform for subject-specific image analysis, visualization, and clinical support *Intraoperative Imaging and Image-Guided Therapy* ed F Jolesz (New York: Springer) pp 277–89

Knäusl B, Fuchs H, Dieckmann K and Georg D 2016 Can particle beam therapy be improved using helium ions?—a planning study focusing on pediatric patients *Acta Oncol.* **55** 751–9

Krämer M, Scifoni E, Schmitz F, Sokol O and Durante M 2014 Overview of recent advances in treatment planning for ion beam radiotherapy *Eur. Phys. J.* D **68** 306

Krämer M *et al* 2016 Helium ions for radiotherapy? Physical and biological verifications of a novel treatment modality *Med. Phys.* **43** 1995–2004

Kurz C, Mairani A and Parodi K 2012 First experimental-based characterization of oxygen ion beam depth dose distributions at the Heidelberg Ion-Beam Therapy Center *Phys. Med. Biol.* **57** 5017–34

Malinen E and Søvik Å 2015 Dose or 'LET' painting—what is optimal in particle therapy of hypoxic tumors? *Acta Oncol.* **54** 1614–22

Schardt D, Elsässer T and Schulz-Ertner D 2010 Heavy-ion tumor therapy: physical and radiobiological benefits *Rev. Mod. Phys.* **82** 383

Schulz-Ertner D, Nikoghosyan A, Didinger B, Münter M, Jäkel O, Karger C P and Debus J 2005 Therapy strategies for locally advanced adenoid cystic carcinomas using modern radiation therapy techniques *Cancer* **104** 338–44

Scifoni E, Tinganelli W, Kraft-Weyrather W, Durante M, Maier A and Krämer M 2013 Including oxygen enhancement ratio in ion beam treatment planning: model implementation and experimental verification *Phys. Med. Biol.* **58** 3871–95

Sokol O *et al* 2017 Oxygen beams for therapy: advanced biological treatment planning and experimental verification *Phys. Med. Biol.* **62** 7798

Tessonnier T, Mairani A, Brons S, Sala P R, Cerutti F, Ferrari A, Haberer T, Debus J and Parodi K 2017 Helium ions at the heidelberg ion beam therapy center: comparisons between FLUKA Monte Carlo code predictions and dosimetric measurements *Phys. Med. Biol.* **62** 6784

Thorwarth D, Eschmann S M, Paulsen F and Alber M 2007 Hypoxia dose painting by numbers: a planning study *Int. J. Radiat. Oncol. Biol. Phys.* **68** 291–300

Tinganelli W, Durante M, Hirayama R, Krämer M, Maier A, Kraft-Weyrather W, Furusawa Y, Friedrich T and Scifoni E 2015 Kill-painting of hypoxic tumours in charged particle therapy *Sci. Rep.* **5** 17016

Tommasino F, Scifoni E and Durante M 2016 New Ions for Therapy *Int. J. Part. Ther.* **2** 428–38

Unkelbach J, Bangert M, De Amorim Bernstein K, Andratschke N and Guckenberger M 2018 Optimization of combined proton–photon treatments *Radiother. Oncol.* **128** 133–8

Unkelbach J, Botas P, Giantsoudi D, Gorissen B L and Paganetti H 2016 Reoptimization of intensity modulated proton therapy plans based on linear energy transfer *Int. J. Radiat. Oncol. Biol. Phys.* **96** 1097–106